RSC Advances

PAPER

View Article Online
View Journal | View Issue

Check for updates

Cite this: *RSC Adv.*, 2023, **13**, 23812

A novel HBI-based ratiometric fluorescent probe for rapid detection of trifluoroborate†

Gao Liang,[a] Zheng Minghao,[b] Liu Haiyi,[c] Xiao Jun,[b] Gong Tianhao,[b] Liu Kunming, *[b] Li Juanhua*[b] and Liu Jinbiao *[b]

A 2-(2′-hydroxyphenyl)benzimidazole (**HBI**)-based ratiometric fluorescent probe, known as **BTEP**, was synthesized using 5-bromosalicylaldehyde as the raw material *via* Sonogashira coupling and condensation reaction. This probe was designed for rapid detection of boron trifluoride solutions and gases. The N and O coordination atoms in the probe undergo a boron difluoride addition with BF_3, which affects the process of excited state intramolecular proton transfer (ESIPT) leading to a blue shift of fluorescence emission. Obvious changes in the fluorescence signal can be observed within 60 seconds. The introduction of an acetylene trimethylsilane fragment increases the conjugate plane and is beneficial to improving the selectivity of the probe. The I_{408}/I_{479} fluorescence ratio of the probe displays a linear relationship with the concentration of BF_3 in the range of 5–50 μM, with a detection of limit as low as 69.5 nM. Furthermore, the probe demonstrates specific and selective recognition of BF_3 among eight common interference substances. Test strips prepared using **BTEP** have the capability of real-time naked-eye detection of trace BF_3 gas.

Received 5th July 2023
Accepted 3rd August 2023

DOI: 10.1039/d3ra04474b

rsc.li/rsc-advances

Open Access Article. Published on 09 August 2023. Downloaded on 5/11/2025 11:19:00 AM.
This article is licensed under a Creative Commons Attribution-NonCommercial 3.0 Unported Licence.

1. Introduction

As an important chemical raw material, trifluoroborate (BF_3) is widely used not only in the synthesis of inorganic and organic boron compounds,[1–3] but also as a Lewis acid catalyst for esterification, alkylation, sulfurization, nitration, and polymerization.[4–8] In addition, BF_3 is also an important precursor for gas phase deposition in the semiconductor industry.[9] However, BF_3 has strong corrosion and toxicity, and even minor leakage can lead to environmental pollution and harm to organisms.[10] Due to its high activity, BF_3 can react with metals, organic substances, and other materials. When exposed to water or moisture, it will explode violently and release hydrogen fluoride gas, causing serious irritation to the respiratory tract, eyes, and skin, and even leading to death.[11] Therefore, developing highly sensitive and rapid response BF_3 detection methods for real-time monitoring during production, transportation, storage, and use is of great significance for environmental protection and human health.

Currently, several detection technologies have been developed, including Fourier transform infrared spectroscopy (FT-TR),[12] quartz crystal microbalance (QCMB),[13] and chemically impregnated test papers.[14] Fluorescent probe are appealing tools in trace pollutant detection due to high sensitivity, simple operation, and obvious signal changes.[15–19] However, the examples of BF_3 fluorescent probes are limited, and mostly obtained through chemical modification of fluorophores such as rhodamine,[20] 1,3-diphenyl-1,3-propanedione (DBM),[21] isobutylene ketone,[22] and coumarin.[23]

As one of the important fluorescent dyes with excited state intramolecular proton transfer (ESIPT) effect, substituted 2-(2′-hydroxyphenyl)benzimidazole (**HBI**) presented superior fluorescent properties such as large fluorescence quantum yields in solution, as compared to oxygen or sulfur analogues.[24] Pariat *et al.* synthesized a series of **HBI** derivatives mono- or bisfunctionalized with ethynyltriisopropylsilane substituents at various positions, demonstrated that the nature of the benzimidazole ring and incorporation of rigid ethynyl-extended moieties at the periphery of the H-bond donor (phenol ring) could afford the fluorophores strong luminescence emission.[25] In addition, the synthesis of imidazolium fluorescent materials is simple, cost-effective, and easy to modify. These advantages make **HBI** have broad application prospects in the field of fluorescent sensing.

In this paper, the **HBI** segment was used as the main structural backbone and ethynyltrimethylsilane (**TMSA**) was introduced in the para site of recognition unit (–OH). A novel probe

[a]*Ganzhou Teacher's College, Ganzhou, Jiangxi 341000, P. R. China*

[b]*Jiangxi Provincial Key Laboratory of Functional Molecular Materials Chemistry, Faculty of Materials Metallurgy and Chemistry, Jiangxi University of Science and Technology, 86 Hongqi Road, Ganzhou 341000, P. R. China. E-mail: liukunming@jxust.edu.cn; lijuanhua@jxust.edu.cn; liujinbiao@jxust.edu.cn*

[c]*Ganzhou No. 3 Middle School, Ganzhou, Jiangxi 341000, China*

† Electronic supplementary information (ESI) available. See DOI: https://doi.org/10.1039/d3ra04474b

© 2023 The Author(s). Published by the Royal Society of Chemistry

Open Access Article. Published on 09 August 2023. Downloaded on 5/11/2025 11:19:00 AM.
This article is licensed under a Creative Commons Attribution-NonCommercial 3.0 Unported Licence.

BTEP for rapidly identifying BF_3 was designed based on the ESIPT mechanism. On the one hand, due to the formation of a larger conjugate plane between the ethynyl group and **HBI** skeleton, the elevation in fluorescent efficiency can help to improve the sensitivity of the probe. On the other hand, the electron-withdrawing properties of the **TMSA** group can be used to adjust the binding ability of the probe with the boron atom, achieving selective recognition of BF_3.

2. Experimental section

2.1 Materials and methods

5-Bromosalicylaldehyde, ethyltrimethylsilane, *o*-phenylenediamine, $PdCl_2(PPh_3)_2$, PPh_3, CuI, trifluoroborate ethyl ether solution, bis(pinacolato)diboron, boric acid, phenylboronic acid, allyl trifluoroborate potassium, hydrogen fluoride, trifluoroacetic acid, potassium fluoride, tetrabutylammonium fluoride and related organic solvents were purchased from Shanghai Aladdin Bio-Chem Technology Co, LTD and used as received.

2.2 General instrumentation

Emission spectra were performed on a Fluorescence spectrometer (F-4600). Error limits were estimated: λ ($\pm$1 nm); τ ($\pm$10%); φ ($\pm$10%). Absorption spectra were recorded on UV-6300 spectrophotometer. IR spectra were recorded on Vario EL III Fourier transform infrared spectrometer (Elementar, Germany). ^{1}H NMR (400 MHz) and ^{13}C NMR (100 MHz) spectra were recorded on Bruker Avance AV400 spectrometer (Bruker, Billerica, MA, USA) unless otherwise noted. The chemical shifts (δ) were quoted in parts per million from tetramethylsilane for ^{1}H and $CDCl_3$ for ^{13}C spectroscopy.

2.3 Synthesis and characterization of BTEP

2.3.1 Synthesis of HTEB. 5-Bromosalicylaldehyde (3.00 g, 15.0 mmol) and ethyltrimethylsilane (2.45 g, 25.0 mmol) were added into a three-necked flask followed by 30 mL of tetrahydrofuran and 20 mL of triethylamine in sequence. Under nitrogen atmosphere, $PdCl_2(PPh_3)_2$ (0.30 g, 0.40 mmol), PPh_3 (0.24 g, 0.80 mmol) and CuI (0.21 g, 1.1 mmol) were added. The reaction was heated under reflux for 4 h. After cooling to room temperature, the reaction mixture was filtered, and washed with 10 mL of ethyl acetate. The filtrate was concentrated under reduced pressure and purified by column chromatography (PE : EA = 40 : 1) to obtained **HTEB** as a light yellow solid (2.86 g, yield of 88%). IR (KBr, cm^{-1}): 3210, 2876, 2150, 1667, 1476, 848; ^{1}H NMR (400 MHz, $CDCl_3$) δ 11.04 (s, 1H), 9.78 (s, 1H), 7.64 (d, J = 2.1 Hz, 1H), 7.53 (dd, J = 8.7, 2.1 Hz, 1H), 6.87 (d, J = 8.7 Hz, 1H), 0.18 (s, 9H); ^{13}C NMR (400 MHz, $CDCl_3$) δ 196.2, 161.6, 140.2, 137.5, 120.4, 118.0, 115.2, 103.2, 93.9, 0.0.

2.3.2 Synthesis of BTEP. **HTEB** (2.18 g, 10.0 mmol) and *o*-phenylenediamine (1.62 g, 15.0 mmol) were added into a three-necked flask, followed by the addition of 25 mL ethanol. After refluxing for 8 h, the reaction solution was concentrated and purified by column chromatography (PE : EA = 40 : 1) to obtain a white solid **BTEP** (2.32 g, yield of 76%). IR (KBr, cm^{-1}): 3288, 2152, 1585, 1498, 1255; ^{1}H NMR (400 MHz, DMSO-d_6) δ 13.62 (s, 1H), 13.36 (s, 1H), 8.27 (d, J = 1.9 Hz, 1H), 7.67–7.72 (m, 2H), 7.30–7.46 (m, 3H), 7.04 (d, J = 8.5 Hz, 1H), 0.25 (s, 9H); ^{13}C NMR (400 MHz, DMSO-d_6) δ 158.0, 156.6, 150.2, 149.8, 140.0, 134.2, 133.5, 129.3, 127.9, 119.0, 117.3, 114.1, 112.4, 104.5, 91.9, 0.5 (Fig. 1).

2.4 Fluorescence detection of BF_3

The experimental details of fluorescent and colorimetric detecting condition optimization were provided in the ESI file.† As for sensitivity testing, **BTEP** (50 μM) and a various concentrations of BF_3 (0–100 μM) were added in a cuvette sequentially. After the above mixed solutions reacted for 60 s, fluorescence spectra were measured and recorded using a Fluorescence spectrophotometer.

The limit of detection (LOD) is calculated according to the following formula:

$$\mathrm{LOD} = 3\sigma/k$$

where σ is the standard deviation of the blank signals (n = 3).

3. Results and discussion

Since most fluorescent materials are sensitive to external environments, we first studied the effect of **BTEP** on BF_3 recognition in different solvent systems. Common organic solvents such as dichloromethane (DCM), acetonitrile (ACN), *N*,*N*-dimethylformamide (DMF) and dimethylsulfoxide (DMSO) were selected as detection solutions, and the fluorescence spectra of probe **BTEP** before and after adding BF_3 were measured. As shown in Fig. 2, the blank probe showed a larger fluorescence intensity in all four solutions. After adding BF_3, there was no significant fluorescence change in

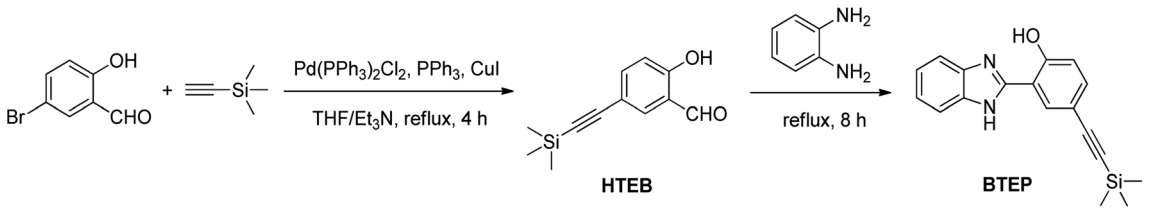

Fig. 1 Synthetic route of target compound BTEP.

Open Access Article. Published on 09 August 2023. Downloaded on 5/11/2025 11:19:00 AM.
This article is licensed under a Creative Commons Attribution-NonCommercial 3.0 Unported Licence.

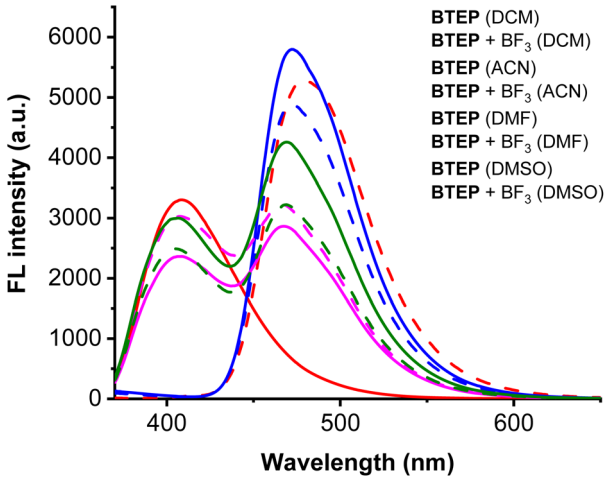

Fig. 2 The effect of **BTEP** (100 μM) on BF_3 (200 μM) response under different solvent conditions, λ_{ex} = 345 nm, rt for 60 s.

the ACN, DMF and DMSO detection systems. However, in the DCM detection solution, the maximum fluorescence emission peak shifted from 479 nm to 408 nm. This significant difference in fluorescence signal helps to accurately determine BF_3, so DCM was chosen as the detection solvent in subsequent experiments.

The response time is an important indicator for the response capability of probe. The alteration of fluorescence against various incubation time was examined. As shown in Fig. 3, the fluorescence intensity at 408 nm can reach the plateau peak within 60 seconds, and fluorescent intensity enhanced upon to 75 times, indicating that the probe has the ability to detect BF_3 in real-time. Hence, the reaction time was selected as 60 seconds in subsequent experiments.

In order to establish the linear relationship between BF_3 concentration and fluorescence intensity, we conducted

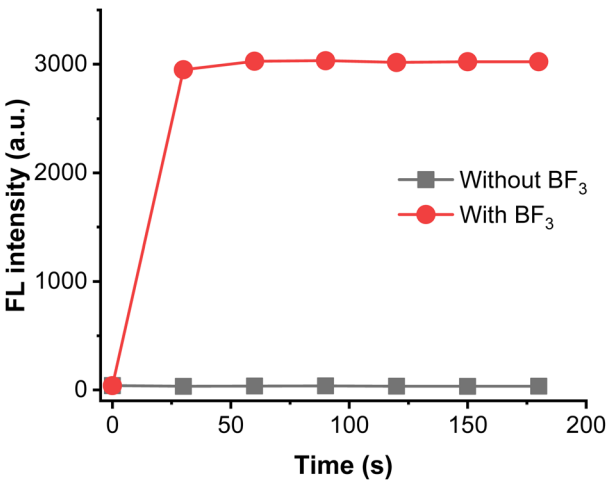

Fig. 3 Time-dependent the fluorescent emission of **BTEP** (100 μM) at 408 nm with BF_3 (200 μM), λ_{ex} = 345 nm.

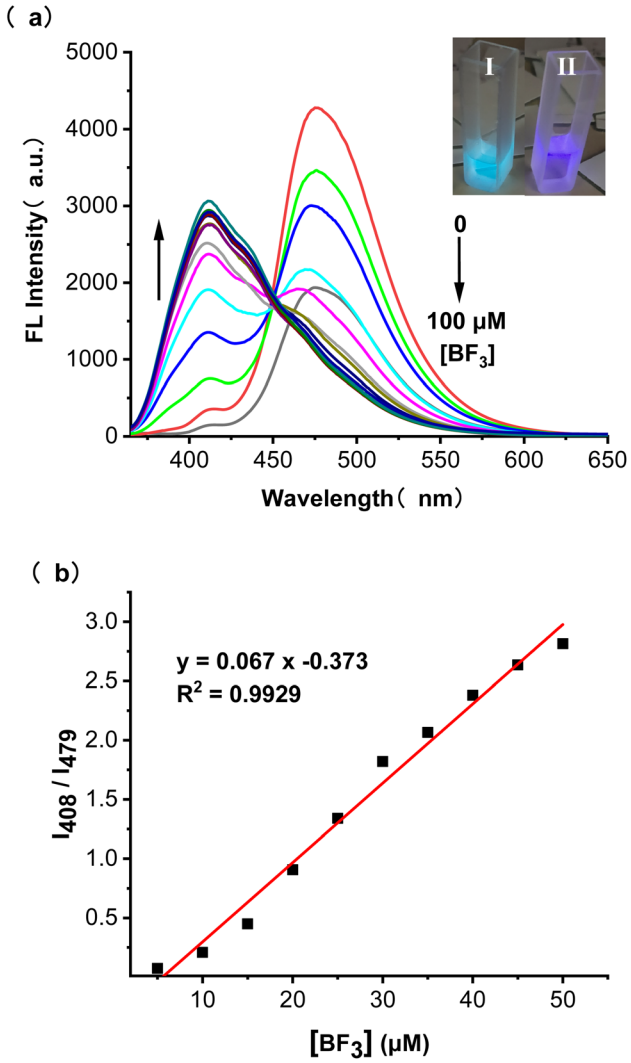

Fig. 4 (a) Fluorescent intensity of **BTEP** (50 μM) upon titration of BF_3 (0–100 μM), λ_{ex} = 345 nm. Inset: photographs of 1 mM of **BTEP** without BF_3 (I), and with 2 mM BF_3 (II) under the 365 UV lamp; (b) the linear correlations between fluorescence intensity ratio and the concentration of BF_3 (5–50 μM), λ_{ex} = 345 nm.

fluorometric titration experiments with different concentrations of BF_3 solutions. The fluorescence spectrum is shown in Fig. 4a. When BF_3 was added, the emission peak at 479 nm of **BTEP** gradually weakened, while a new emission peak appeared at 408 nm and its intensity gradually increased. The ratio of the intensity of the two emission peaks (I_{408}/I_{479}) to the concentration of BF_3 was plotted, and it was found that there was a good linear relationship at a concentration range of 5–50 μM BF_3, resulting in a linear equation of $I_{408}/I_{479} = 0.067[BF_3] - 0.373$ ($R^2 = 0.9929$). A limit of detection (LOD) was calculated as low as 69.5 nM limit according to LOD = $3\sigma/k$ (where σ is the standard deviation of blank measurement, k is the slope between the fluorescence intensity *versus* BF_3 concentration) (Fig. 4b). Additionally, under ultraviolet light, it can be observed that the probe solution changed from light blue to dark blue before and

© 2023 The Author(s). Published by the Royal Society of Chemistry

Open Access Article. Published on 09 August 2023. Downloaded on 5/11/2025 11:19:00 AM.
This article is licensed under a Creative Commons Attribution-NonCommercial 3.0 Unported Licence.

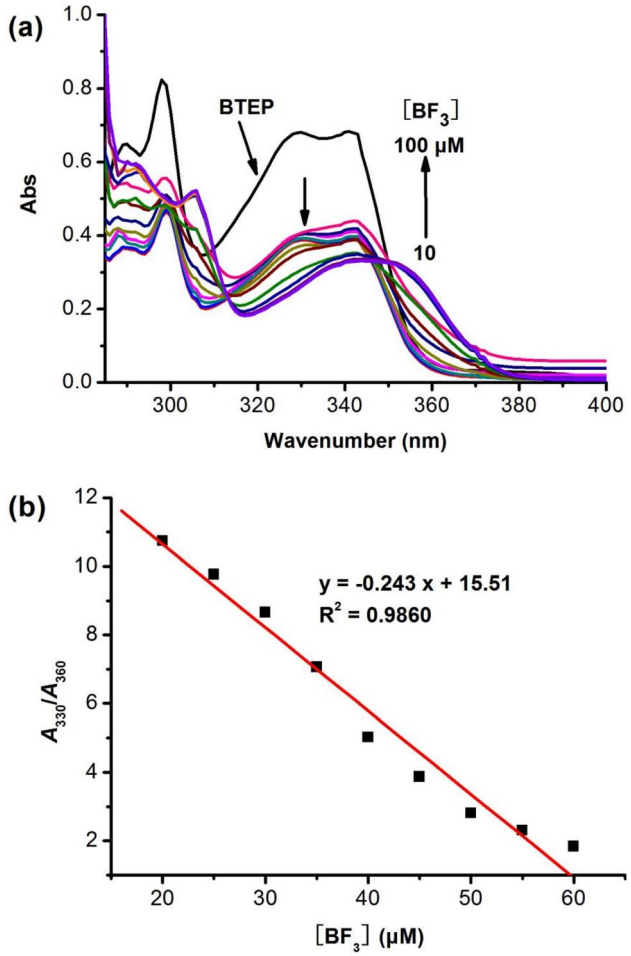

Fig. 5 (a) The UV-vis spectra of **BTEP** (50 μM) upon titration of BF_3 (10–100 μM); (b) the linear correlations between absorbance intensity ratio of 330 nm/360 nm and the concentration of BF_3 (20–60 μM).

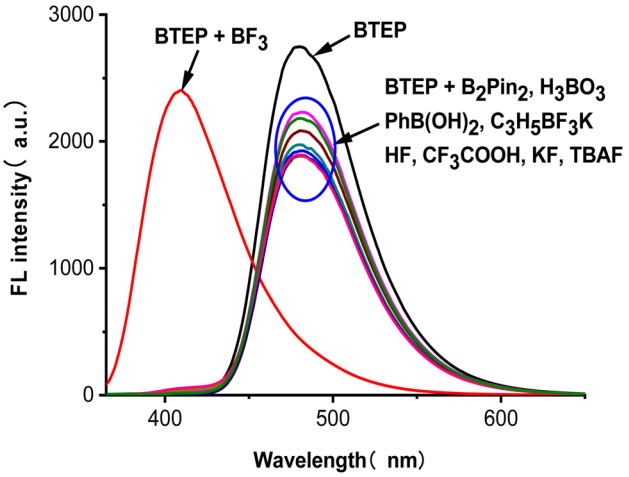

Fig. 6 Fluorescent spectra of **BTEP** (50 μM) with various interferences (50 μM), $\lambda_{ex} = 345$ nm.

after adding BF_3, demonstrating the naked-eye recognition potential of the probe.

The effect of adding BF_3 on the absorption behaviour of **BTEP** was also investigated. DCM was found to be the most suitable solution for selective colorimetric detection of BF_3 (Fig. S7†). The **BTEP** has a distinct absorption peak at 330 nm in UV-vis spectrum, which gradually disappeared with increasing the concentration of BF_3. Simultaneously, the absorption at 360 nm occurred and increased significantly (Fig. 5a). The probe **BTEP** exhibited an excellent linearity between the absorbance ratio (A_{330}/A_{360}) and the concentration of BF_3 from 20 to 60 μM, $R^2 = 0.9860$ (Fig. 5b). Thus, **BTEP** could be promising as a naked eye colorimetric sensor for BF_3 detection.

High selectivity to analyte over potentially competing species is an important indicator for the anti-interference capability of probe. To examine the selectivity of **BTEP**, we chose eight common borates and fluorides to add to the probe solution and performed fluorescence spectra measurements. As shown in Fig. 6, the addition of common borates and fluorides such as bis(pinacolato)diboron, boric acid, phenylboronic acid, allyl trifluoroborate potassium, hydrogen fluoride, trifluoroacetic acid, potassium fluoride, and tetrabutylammonium fluoride only resulted in a slight decrease of fluorescence. Nevertheless, the addition of BF_3 leaded to a significant blue shift in the fluorescent emission peak, indicating that **BTEP** has a specific recognition ability for BF_3.

The addition of BF_3 to the N, O ligand atoms in a typical ESIPT molecule such as 2-(2′-hydroxyphenyl)benzothiazole (HBT), the C–C bond configuration connecting the benzothiazole and phenol moieties will be locked. This process is often accompanied by a significant difference in fluorescence signal.[26,27] The ^{1}H NMR spectra of **BTEP** before and after the addition of BF_3 shows in Fig. 7. The most significant change is the disappearance of the peaks at 13.36 ppm and 13.62 ppm, accompanied by the emergence of peak at 11.71 ppm, which is due to the addition between BF_3 and hydroxyl groups of **BTEP**. This process also affects the chemical shift of –NH in benzimidazole unit. Therefore, it can be indicates that the blue shift of fluorescent emission is caused by the formation of **BTEP**–BF_2 adducts.

Given the high sensitivity, selectivity, and rapid response ability of probe **BTEP** for detecting trifluoroborate ethyl ether solution, we have prepared a test strip based on it and attempted to use it for naked-eye identification of BF_3 gas. The test strip was encapsulated in different concentrations of BF_3 vapor as shown in Fig. 8. Under UV light at 365 nm, the test strip emitted bright blue fluorescence. At room temperature, the test strip responded quickly within 5 minutes for BF_3 gas concentrations within the range of 10 μM to 10 mM. As the concentration of BF_3 gas increased, the test strip gradually changed from bright blue to deep blue fluorescence through naked-eye observation, indicating that the **BTEP** test strip has potential application value for real-time early warning of trace BF_3 gas in the environment.

© 2023 The Author(s). Published by the Royal Society of Chemistry

Open Access Article. Published on 09 August 2023. Downloaded on 5/11/2025 11:19:00 AM.
This article is licensed under a Creative Commons Attribution-NonCommercial 3.0 Unported Licence.

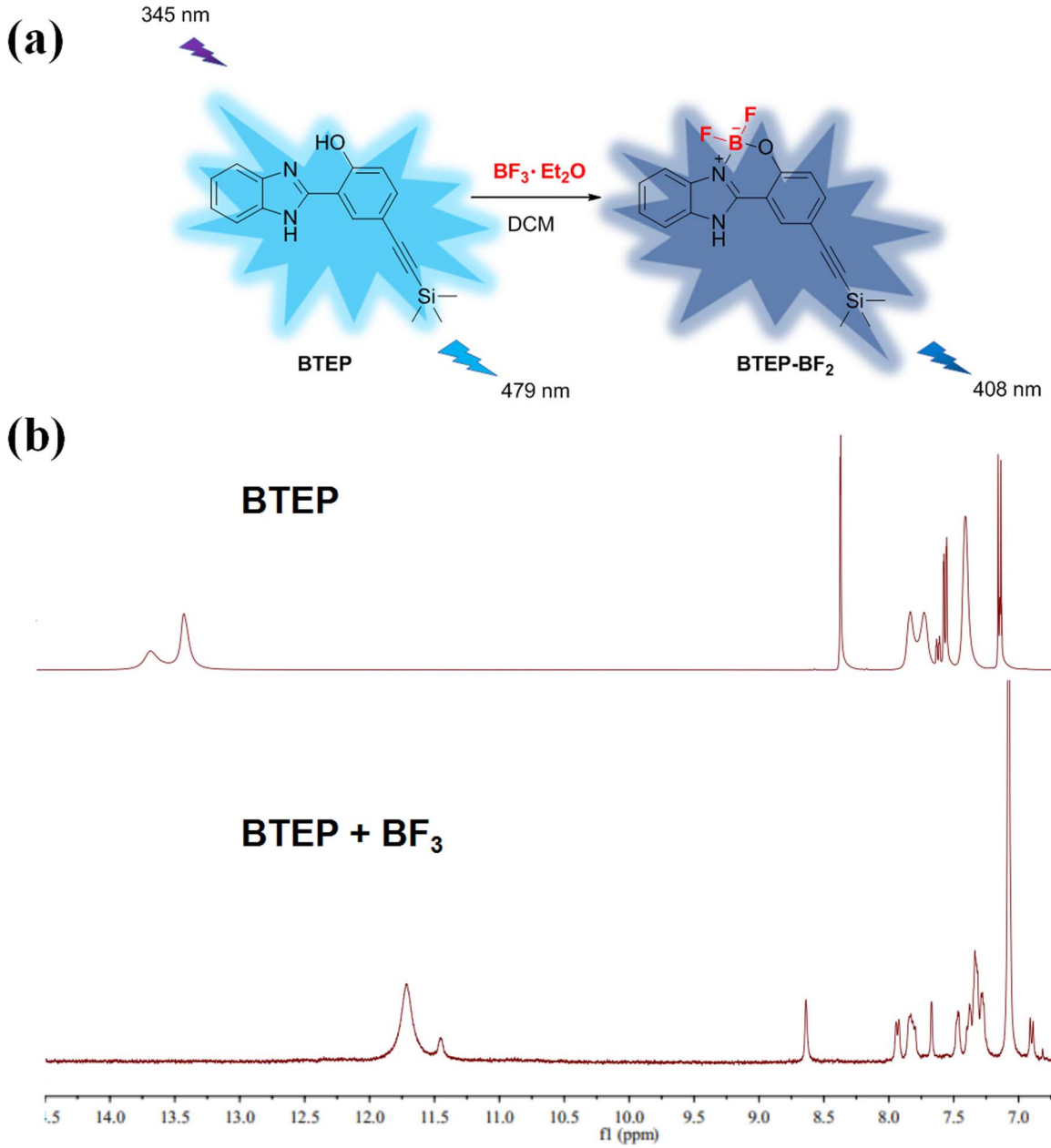

Fig. 7 (a) Proposed detection mechanism; (b) ^{1}H NMR spectra of **BTEP** before and after the addition of BF_3.

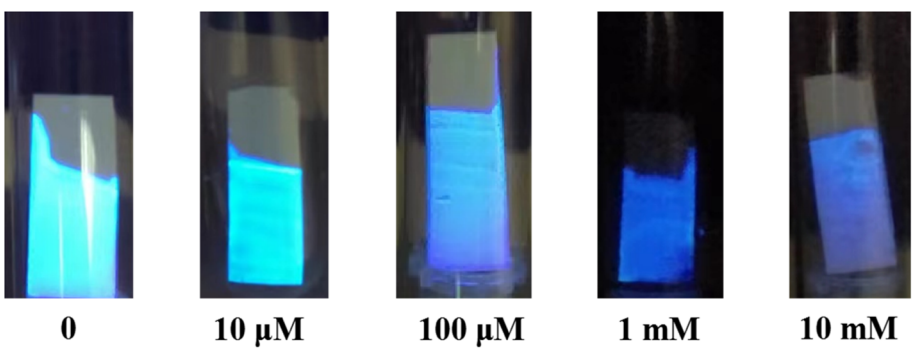

Fig. 8 Photographs of fluorescent response of **BTEP** test strips in the different concentrations of BF_3 gas.

© 2023 The Author(s). Published by the Royal Society of Chemistry

Open Access Article. Published on 09 August 2023. Downloaded on 5/11/2025 11:19:00 AM.
This article is licensed under a Creative Commons Attribution-NonCommercial 3.0 Unported Licence.

4. Conclusions

In this work, a rapid ratiometric fluorescent probe **BTEP** for the selective detection of BF_3 has been synthesized. By forming a BF_2 adduct in the **HBI** skeleton through the coordination of N and O atoms with BF_3, the ESIPT process of the probe is affected, resulting in blue shift of fluorescence emission. Within a range of 5–50 μM concentration of BF_3 in dichloromethane solution, the linear increase of fluorescence ratio at I_{408}/I_{479} exhibits LOD as low as 69.5 nM. The absorbance response of BF_3 at **BTEP** was linear in the wide range of 20–60 μM. Additionally, test strips for real-time naked-eye identification of BF_3 gas have been prepared.

Conflicts of interest

The authors declare that they have no known competing financial interests or personal relationships that could have appeared to influence the work reported in this paper.

Acknowledgements

Financial support from the Jiangxi Provincial Natural Science Foundation (20212BAB203013), the Science and Technology Project Founded by the Education Department of Jiangxi Province (GJJ2200820, GJJ181187), National College Students' Innovation and Entrepreneurship Training Program (202110407006) is gratefully acknowledged.

References

1 K. Chansaenpak, M. Z. Wang, H. Wang, B. C. Giglio, F. P. Gabbaï, Z. H. Wu and Z. Li, *RSC Adv.*, 2017, **7**, 17748–17751.
2 N. An, H. Pi, L. Liu, W. Du and W. Deng, *Chin. J. Chem.*, 2011, **29**, 947–950.
3 B. Köksoy, E. N Kaya, F. Hacıvelioğlu, S. Yeşilot and M. Durmuş, *Dyes Pigm.*, 2017, **140**, 384–391.
4 S. Sultana, S. M. B. Maezono, M. S. Akhtar, J. Shim, Y. Wee, S. H. Kim and Y. R. Lee, *Adv. Synth. Catal.*, 2018, **360**, 751–761.
5 P. Costa, I. Trosien, J. Mieres-Perez and W. Sander, *J. Am. Chem. Soc.*, 2017, **139**, 13024–13030.
6 M. M. Huang, L. Z. Hu, S. Hang, Q. Liu, M. I. Hussain, J. Pan and Y. Xiong, *Green Chem.*, 2016, **18**, 1874–1879.
7 X. G. Yang, K. K. Wu and Z. K. Yu, *Tetrahedron Lett.*, 2015, **56**, 4490–4493.
8 H. Shen, J. Li, Q. Liu, J. Pan, R. F. Huang and Y. Xiong, *J. Org. Chem.*, 2015, **80**, 7212–7218.
9 S. Gene, G. Gordon, P. Timothy and S. Michael, *J. Mater. Res.*, 2018, **33**, 4233–4240.
10 G. M. Rusch, G. M. Hoffman, R. F. McConnell and W. E. Rinehart, *Toxicol. Appl. Pharmacol.*, 1986, **83**, 69–78.
11 Y. Minoru, T. Kazuhiro, I. Keisuke, G. Kenta, T. Fumito and O. Hideki, *Photochem. Photobiol. Sci.*, 2019, **18**, 2884–2892.
12 M. M. Roshani, E. Rostaminikoo, E. Joonaki, A. M. Dastjerdi, B. Najafi, V. Taghikhani and A. Hassanpouryouzband, *Fuel*, 2022, **313**, 122998.
13 Y. M. Liu, J. Y. Zhang, Y. Z. Wang, C. Y. Liu, G. L. Zhang and W. S. Liu, *Sens. Actuators, B*, 2017, **243**, 940–945.
14 B. A. Denenberg and R. Kriesel, *Am. Ind. Hyg. Assoc. J.*, 1976, **37**, 246–250.
15 Q. X. Ye, S. F. Ren, H. Huang, G. G. Duan, K. M. Liu and J. B. Liu, *ACS Omega*, 2020, **5**, 20698–20706.
16 L. Q. Li, M. H. Zheng, X. Y. Yan, H. Huang, S. X. Cao, K. M. Liu and J. B. Liu, *J. Photoch. Photobio. A-Chem.*, 2022, **432**, 114069.
17 D. D. Jiang, M. H. Zheng, X. Y. Yan, B. Huang, H. Huang, T. H. Gong, K. M. Liu and J. B. Liu, *RSC Adv.*, 2022, **12**, 31186–31191.
18 L. Q. Li, M. H. Zheng, D. D. Jiang, S. X Cao, K. M. Liu and J. B. Liu, *Prog. Chem.*, 2022, **34**, 1815–1830.
19 C. T. Shi, Z. Y. Huang, A. B. Wu, Y. X. Hu, N. C. Wang, Y. Zhang, W. M. Shu and W. C. Yu, *RSC Adv.*, 2021, **11**, 29632–29660.
20 Y. Z. Wang, Y. Yang, F. Z. Qiu, Y. Feng, X. R. Song, G. l. Zhang and W. S. Liu, *Sens. Actuators, B*, 2018, **276**, 166–172.
21 P. Banet, L. Legagneux, P. Hesemann, J. Moreau, L. Nicole, A. Quach, C. Sanchez and T. Tranthi, *Sens. Actuators, B*, 2008, **130**, 1–8.
22 Z. L. Wang, Y. Zhang, J. Song, Y. Y. Wang, M. X. Li, Y. Q. Yang, X. Xu, H. J. Xu and S. F. Wang, *Sens. Actuators, B*, 2020, **304**, 127083.
23 H. Zhao, T. Wu, Y. Sun, L. Duan and Y. Ma, *Chem. Res. Chin. Univ.*, 2021, **42**, 2422–2427.
24 S. K. Behera, G. Sadhuragiri, P. Elumalai, M. Sathiyendiran and G. Krishnamoorthy, *RSC Adv.*, 2016, **6**, 59708–59717.
25 T. Pariat, M. Munch, M. Durko-Maciag, J. Mysliwiec, P. Retailleau, P. M. Vérité, D. Jacquemin, J. Massue and G. Ulrich, *Chem.–Eur. J.*, 2021, **27**, 3483–3495.
26 V. S. Padalkar and S. Seki, *Chem. Soc. Rev.*, 2016, **45**, 169–202.
27 X. Li and Y. A. Son, *Dyes Pigm.*, 2014, **107**, 182–187.

© 2023 The Author(s). Published by the Royal Society of Chemistry